TOXICOLOGICAL SCIENCES **75,** 368–377 (2003)
DOI: 10.1093/toxsci/kfg195

Effects of Inorganic $HgCl_2$ on Adipogenesis

David M. Barnes,*,†,[1] Paul R. Hanlon,†,‡,[2] and Emily A. Kircher*,†,[2]

*Department of Animal Sciences, †Department of Molecular and Environmental Toxicology, and ‡Department of Pharmacology, University of Wisconsin, Madison, Wisconsin 53706

Received May 10, 2003; accepted July 7, 2003

Mercury is a common pollutant that alters glucose metabolism in adipocytes; however, the effect of $HgCl_2$ on differentiating adipocytes and their subsequent metabolic function is not well understood. Two adipocyte models, the 3T3-L1 and C3H10T1/2 (10T1/2) cell lines, were differentiated in the presence of $HgCl_2$. To assess the amount of differentiation in a population, markers of differentiation (i.e., PPARγ and GLUT 4 expression and lipid accumulation) and functions of adipocytes (i.e., glucose transport and insulin-induced glucose transport) were measured. $HgCl_2$ exposure significantly decreased the number of phenotypic adipocytes and PPARγ expression in both 3T3-L1 and 10T1/2 cells without effects on cell viability. GLUT 4 was significantly reduced by $HgCl_2$ treatment in 10T1/2 but not 3T3-L1 cells. Exposure to $HgCl_2$ during differentiation increased basal glucose uptake in a dose-dependent manner (up to 2.5-fold) and decreased insulin-induced glucose uptake in 3T3-L1 adipocytes. In contrast, $HgCl_2$ had little effect on basal or insulin-induced glucose uptake in 10T1/2 cells, possibly due to their lower insulin responsiveness. We examined the effect of $HgCl_2$ exposure on signaling event involved in differentiation of adipocytes and cellular stress, namely, the phosphorylation of ERK1/2 and JNK, respectively. $HgCl_2$ exposure had no effect on ERK1/2 phosphorylation in either cell line, increased JNK phosphorylation in the 10T1/2, and had no effect on JNK phosphorylation in 3T3-L1 cells. These data indicate $HgCl_2$ exposure can inhibit the differentiation of fibroblasts into adipocytes as well as influence signaling events and the subsequent metabolic activity of differentiated adipocytes.

Key Words: **adipocyte; adipogenesis; mercury; differentiation; 3T3-L1; 10T1/2**

Terminal differentiation of precursor cells into adipocytes is an important component of glucose and lipid metabolism throughout the development and life of animals. Thus, disruption of differentiation may result in serious developmental and adult diseases related to glucose/lipid metabolism. *In vitro* research has shown that adipocyte differentiation and/or metabolism is disrupted by exposure to numerous environmental chemicals, such as dioxin and endrin, and metal contaminants, such as arsenite, vanadate, and the Group IIb metals: Cd^{2+}, Zn^{2+}, and Hg^{2+} (Alexander *et al*., 1998; Barnes *et al*., 1999; Ezaki, 1989; Jin *et al*., 2000; Liao and Lane, 1995; Moreno-Aliaga and Matsumura, 2000; Wauson *et al*., 2002).

Metals have been shown to have a wide variety of effects on adipocytes. Vanadate inhibits adipocyte differentiation of the preadipocyte 3T3-L1 cell line when added during the first 24 h of differentiation (Jin *et al*., 2000; Liao and Lane, 1995). Vanadate also stimulates glucose transport and lipogenesis in rat adipocytes (Dubyak and Kleinzeller, 1980; Shechter and Ron, 1986). Arsenite inhibits adipocyte differentiation of the C3HT101/2 fibroblast cell line with both chronic and acute exposure (Trouba *et al*., 2000; Wauson *et al*., 2002). Zinc increased both glucose transport and phosphorylation of Akt, a kinase involved in the insulin signaling leading to increased glucose transport (May and Contoreggi, 1982; Tang and Shay, 2001). Similarly, studies have shown that low micromolar concentrations of cadmium can increase GLUT 1–mediated glucose uptake in 3T3-L1 adipocytes (Harrison *et al*., 1991). Ezaki (1989) showed a 4-fold stimulation of glucose transport in primary rat adipocytes due to acute exposure to 100 μM $HgCl_2$, while we have found similar effects in 3T3-L1 adipocytes with chronic exposure to low concentrations of $HgCl_2$ (1–10 μM; Barnes and Kircher, unpublished data). Despite the clear effect of metals on adipocytes, the specific impact of $HgCl_2$ on cellular differentiation and subsequent metabolic function of adipocytes remains unclear.

In vitro experiments have shown that terminal adipocyte differentiation has two distinct phases: a commitment phase and a maturation phase (Shao and Lazar, 1997; Xue *et al*., 1996). Cascades of transcription factors, including peroxisome proliferator-activated receptor γ (PPARγ) and the CCAAT/enhancer-binding proteins (C/EBPs), control these two phases. Insulin responsiveness of adipocytes is a characteristic that is acquired during the maturation phase of differentiation (Resh, 1982) and involves the expression of the proteins responsible for the functions of adipocytes (e.g., lipogenesis and insulin-sensitive glucose transport). The ability of adipocytes to respond to insulin is an important component of whole body glucose and lipid metabolism and storage. A decrease in insulin-mediated responses from insulin target tissues is termed

[1] To whom correspondence should be addressed at Department of Animal Sciences, University of Wisconsin-Madison, 2015 Linden Drive, Madison, WI 53706. Fax: (608) 262-5157. E-mail: barnes@calshp.cals.wisc.edu.

[2] Authors contributed equally to this work.

insulin resistance and is an important characteristic of Type II diabetes (Zimmet *et al*., 2001).

In this study, we used the well-characterized 3T3-L1 preadipocyte and the multipotent C3H10T1/2 fibroblast cell models to determine the effects of inorganic $HgCl_2$ on adipocyte differentiation and function. Our results demonstrate that inorganic $HgCl_2$ exposure inhibits differentiation, but not viability, of both cell lines. In addition, we show that $HgCl_2$ treatment decreases the expression of several adipocyte-specific proteins, affects kinases involved in insulin signaling, and decreases insulin-mediated glucose uptake in the 3T3-L1 cell line. The reduction in adipocyte differentiation and subsequent decrease in insulin-mediated glucose transport following $HgCl_2$ exposure suggest that $HgCl_2$ may contribute to insulin resistance and the onset of diseases related to insulin responsiveness.

MATERIALS AND METHODS

Reagents. For the culture of 10T1/2 cells, Dulbecco's modified Eagles medium (DMEM) formulated with F12 media was obtained from Gibco/Invitrogen (Carlsbad, CA) and fetal bovine serum (FBS) was purchased from Atlanta Biological (Norcross, GA). For the culture of 3T3-L1 cells, DMEM was obtained from Sigma Chemical Co. (St. Louis, MO) and FBS and new calf serum (NCS) were obtained from Biowhittaker (Walkersville, MD). Other cell culture reagents for both cell lines were the same and include: bovine pancreatic insulin (28 U/mg), mercuric chloride, dexamethasone, and 3-isobutyl-1-methylxanthine (IBMX), which were purchased from Sigma Chemical Co. [^{3}H]-deoxyglucose (DG, >30 Ci/mmol) was obtained from NEN Life Science Products, Inc. (Boston, MA). Viability of treated and untreated cells was assessed by the release of lactate dehydrogenase using the CytoTox-ONE kit from Promega (Madison, WI) and the manufacturer's recommended protocol. All other chemicals were reagent grade or higher and obtained from commercial sources.

Differentiation of 3T3-L1 cells. 3T3-L1 fibroblasts obtained from ATCC (Rockville, MD) were grown to confluence in high-glucose DMEM containing 10% NCS. Differentiation of 3T3-L1 fibroblasts was performed as described previously with minor modifications (Frost and Lane, 1985). Briefly, the confluent cells were incubated 3 days in DMEM containing 10% FBS, 1 μg/ml insulin, 0.25 μM dexamethasone, and 500 μM IBMX (IDM). Cells were then incubated for an additional 2 days in DMEM containing 10% FBS and 1 μg/ml insulin. After differentiation, adipocytes were maintained in DMEM containing 10% FBS. Visual assessment of lipid droplet formation indicated that > 80% of the cells exhibited the adipocyte phenotype.

Differentiation of C3H10T1/2 cells. C3H10T1/2 cells (ATCC) were maintained in DMEM:F12 media and differentiated as described previously (Phillips *et al*., 1995). Upon reaching confluence, cells were induced to differentiate in DMEM:F12 supplemented with 10% FBS and 10 μg/ml insulin, 1 μM dexamethasone, 0.5 μM IBMX, and 1 μM BRL49653 (IDM/BRL) for 2 days. Cells were then incubated for an additional 5 days in DMEM containing 10% FBS and 10 μg/ml insulin. Differentiation, as assessed by lipid droplet formation, ranged from 30–50%.

Flow cytometry and cell staining. Cells were differentiated in the presence or absence of $HgCl_2$. After differentiation, cells were lifted from the plate with trypsin and fixed with paraformaldehyde (1% final concentration). Nile Red dissolved in DMSO was added to a final concentration of 0.25 μg/ml and staining was quantified by flow cytometry. Cellular Nile Red fluorescence, a measure of lipid accumulation within adipocytes, was measured at 530 nm on a FACSCalibur dual-laser flow cytometer (Becton Dickinson, San Jose, CA). The adipocyte population was identified based on Nile Red staining (lipid content) and side scatter (cell complexity). Data was acquired and analyzed with CellQuest software (Becton Dickinson). For Oil Red O staining and extraction, cells were washed one time with 37°C PBS and incubated with formalin (10% formaldehyde, 90% PBS) for 15 min to fix the cells. After fixing, cells were washed three to four times with tap water. Oil Red O solution (5 mg Oil Red O/ml isopropanol) was added to each well and incubated at room temperature for 2 h. Plates were rinsed three to four times with tap water and allowed to air dry. To extract Oil Red O, isopropanol was added to each well and shaken at room temperature for 5 min, and a sample was read at 510 nm. Oil Red O binds neutral lipids and was used to determine relative amounts of lipid in treated and untreated adipocyte populations for confirmation of Nile Red data. Oil Red O measures total lipid content of all cells in the population rather than just the adipocyte population measured by flow cytometry and Nile Red.

Glucose transport. Glucose uptake was measured 7 days after initiation of the differentiation protocol. Cells were washed twice with KRPH buffer (5 mM Na_2HPO_4, 20 mM HEPES, 1 mM $MgSO_4$, 1 mM $CaCl_2$, 4.7 mM KCl, 0.1% BSA, pH 7.4) and then incubated for 1 h in KRPH buffer. Glucose uptake was measured in the presence and absence of 10 μM cytochlasin B to determine effects on mediated and nonmediated DG uptake. Glucose uptake was measured during the final 10 min by the addition of [^{3}H]-2-deoxyglucose to a final assay concentration of 50 μM DG containing 0.5 μCi 2-[^{3}H]-deoxyglucose/ml. Cells were washed three times in cold PBS, solubilized in 0.5 N NaOH, and aliquots were subjected to scintillation counting. Total protein levels were determined using the Bradford protein assay (Bio-Rad, Hercules, CA).

Immunoblotting. Monoclonal anti-PPARγ, polyclonal anti-GLUT 4, monoclonal antiphospho-ERK, and the appropriate HRP-conjugated antibodies were purchased from Santa Cruz Biotechnology (Santa Cruz, CA). Phospho-specific antibodies raised against JNK were purchased from Upstate Biotechnology (Lake Placid, NY). Equal amounts of protein were separated by SDS-PAGE using 10% polyacrylamide gels and then transferred to ECL nitrocellulose membrane (Amersham, Peapack, NJ), per the manufacturer's protocol. Immunoblotting was performed and proteins were visualized using the HRP-conjugated secondary antibody and ECL detection reagents, per the manufacturer's protocol (Amersham). Blots were scanned and the analysis performed on a Macintosh G4 computer using the public domain NIH Image (version 1.61, developed at the U.S. NIH and available at http://rsb.info.nih.gov/nih-image/).

Statistical analysis. Data were analyzed by one-way analysis of variance (ANOVA, InStat version 2.03). Differences among data means were assessed using a Student-Newman-Keuls multiple comparison test ($p < 0.05$). Experiments were replicated at least three times with representative experiments shown in the figures.

RESULTS

$HgCl_2$ Treatment Inhibits Adipocyte Differentiation in a Dose-Dependent Manner

$HgCl_2$ treatment reduced the number of 10T1/2 and 3T3-L1 cells that acquired the adipocyte phenotype when treated with the hormonal mixture required for differentiation (IDM/BRL and IDM, respectively). The number of adipocytes was quantitated using flow cytometric analysis of the size, complexity, and amount of Nile Red staining of cells. The addition of $HgCl_2$ from the initiation of IDM treatment through 7 days reduced the number of 3T3-L1 cells that became adipocytes in a dose-dependent manner. Treatment with 5–10 μM $HgCl_2$ reduced the number of phenotypic adipocytes by 40–60% (Fig. 1A). The addition of $HgCl_2$ reduced the number of 10T1/2 cells that become adipocytes by 60–90%, with a maximum effect at 10 μM $HgCl_2$ (Figs. 1A and 1B). Lactate

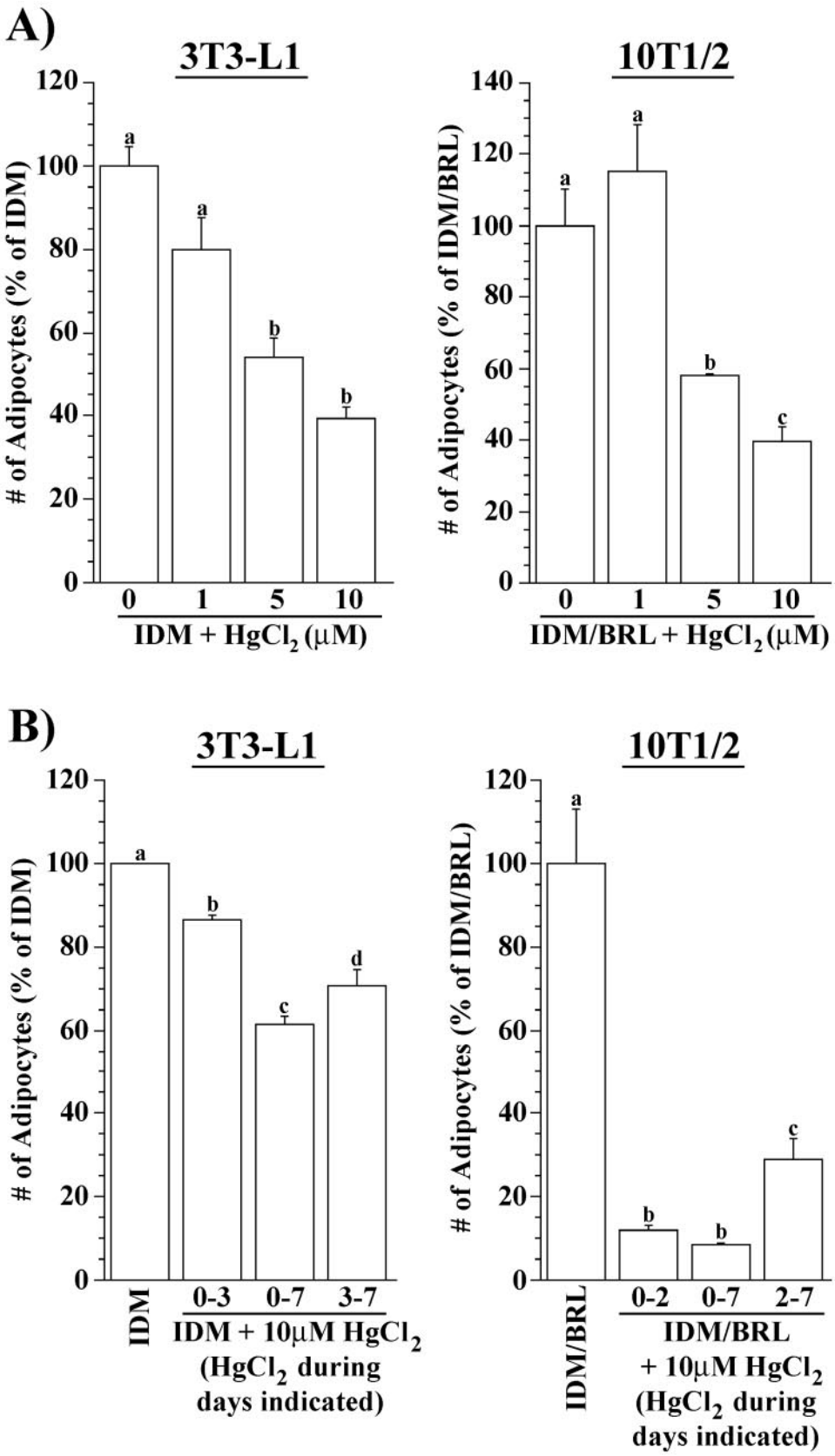

FIG. 1. The effect of $HgCl_2$ on the formation of phenotypic adipocytes as shown by (A and B) representative experiments in which (A) 3T3-L1 and 10T1/2 cells were induced to differentiate as described in Materials and Methods. 3T3-L1 cultures were treated with 1, 5, or 10 μM $HgCl_2$ throughout differentiation and 10T1/2 cultures treated for days 0–2. (B) 3T3-L1 and 10T1/2 cells were induced to differentiate in the presence or absence of 10 μM $HgCl_2$ for the commitment phase, maturation phase, or entire differentiation according to differentiation protocols described in the Materials and Methods. (A and B) 3T3-L1 and 10T1/2 cells were cultured for 7 days after initial hormonal stimulation, fixed, stained with Nile Red, and analyzed by flow cytometry to determine the number of phenotypic adipocytes. Cell complexity and the extent of Nile Red staining were used as criteria for distinguishing the adipocyte population. Results are normalized to IDM or IDM/BRL-stimulated levels (set to 100) and are presented as the mean of four samples ± SEM. Columns with different letters (abc) are significantly different from one another (ANOVA, $p < 0.05$).

dehydrogenase activity was measured to determine the effects of treatment on cell viability. Media LDH was not different from control for 1–20 μM $HgCl_2$, although 50 μM $HgCl_2$ increased media LDH in both cell lines (data not shown). In other experiments, differentiated adipocytes were incubated with 1–10 μM $HgCl_2$ for 16 days without an effect on cell number (Barnes and Kircher, unpublished data).

The magnitude of the inhibition of adipogenesis by $HgCl_2$ varied among experiments and is probably due to differences in passage number and cellular responsiveness to the differentiation cocktail. For example, the percentage of differentiation under control conditions varied among cultures (75–95% and 20–50% for 3T3-L1 and 10T1/2 cells, respectively). However, despite the variability among cultures, we observed consistent and repeatable effects of $HgCl_2$ on adipogenesis in both 3T3-L1 and 10T1/2 cells.

To determine if $HgCl_2$ was effective at a particular stage of differentiation, cells were incubated with $HgCl_2$ for the commitment phase (time exposed to IDM or IDM/BRL), the maturation phase (rest of differentiation), or during the entire differentiation process. Figure 1B shows that 3T3-L1 and 10T1/2 cells differ in their sensitivity to $HgCl_2$ at different phases of differentiation. Mercury inhibited differentiation at all stages, however, the magnitude of inhibition differed among stages. In 3T3-L1 cells, 10 μM $HgCl_2$ treatment was slightly less effective at inhibiting adipogenesis when added during the maturation phase (days 3 to 7) than when $HgCl_2$ was present for the entire differentiation period (Fig. 1B). In 10T1/2 cells, 10 μM $HgCl_2$ exposure during the commitment phase was as effective at inhibiting adipocyte differentiation as if $HgCl_2$ was present throughout differentiation (Fig. 1B). For this reason, in the subsequent experiments, 10T1/2 cells were only exposed to $HgCl_2$ during the commitment phase of differentiation (days 0–2). Exposure of 10T1/2 cells to $HgCl_2$ during only the maturation phase significantly inhibited adipocyte differentiation, although to a lesser degree than the other exposure periods.

$HgCl_2$ Treatment Decreases the Lipid Content of 3T3-L1- and 10T1/2-Derived Adipocytes

The effect of $HgCl_2$ on lipid accumulation (an important component of adipocyte differentiation) in 3T3-L1 and 10T1/2 cells is shown in Figure 2. Cells were exposed to $HgCl_2$ during differentiation and the amount of Oil Red O staining was determined after 8 days. Oil Red O staining can be used to assess the amount of lipid in a population of cells. $HgCl_2$ treatment resulted in a dose-dependent decrease in cellular lipid accumulation in both cell lines (decreased in Oil Red O staining). Oil Red O staining was significantly reduced with 20 μM $HgCl_2$ and 5 μM $HgCl_2$ in 3T3-L1 and 10T1/2 cells, respectively. Using flow cytometry and Nile Red staining, lipid accumulation within individual 3T3-L1 adipocytes was measured. As expected, $HgCl_2$ decreased the average lipid content of differentiated 3T3-L1 adipocytes in a dose-dependent manner (Table 1). Nile Red staining is a more sensitive method for measuring lipid accumulation. Using this more sensitive analysis of lipid accumulation, we observed a decrease in lipid accumulation with 1 μM $HgCl_2$ as compared to 20 μM $HgCl_2$ with Oil Red O staining. Mean Nile Red fluorescence decreased 43% in 3T3-L1 adipocytes exposed to 10 μM $HgCl_2$.

$HgCl_2$ Inhibits Expression of Adipogenic Proteins

To further examine the effects of $HgCl_2$ on adipogenesis, we examined the expression of early (PPARγ) and late (GLUT 4) adipogenic proteins in treated and untreated cells. Peak expression of PPARγ occurs about 48 h after the induction of differentiation and is often used as a marker of early adipocyte

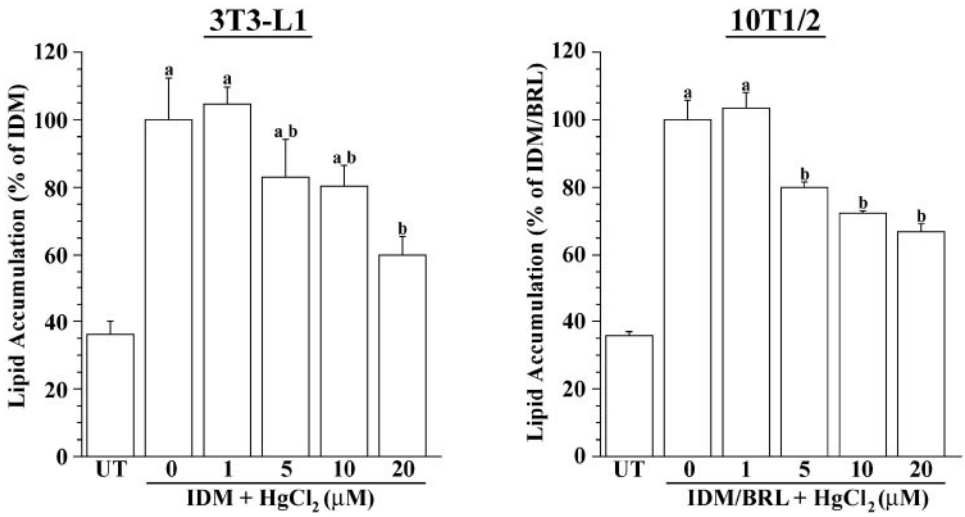

FIG. 2. The effect of $HgCl_2$ on lipid accumulation in 3T3-L1 and 10T1/2 adipocytes as shown by a representative experiment where 3T3-L1 and10T1/2 cells were differentiated in the presence of 0, 1, 5, 10, and 20 μM $HgCl_2$. Following differentiation, cells were fixed with paraformaldehyde and stained with Oil Red O. Stained cells were extracted with isopropanol and cellular Oil Red O, determined by absorbance at 510 nm. Results were normalized to IDM or IDM/BRL-stimulated levels (set to 100). Values presented are the mean of four samples $\pm$ SEM. Columns with different letters (abc) are significantly different from one another (ANOVA, $p < 0.05$).

TABLE 1
Effect of $HgCl_2$ on Lipid Accumulation in 3T3-L1 Adipocytes

μM $HgCl_2$	Nile Red mean fluorescence
0	157.7 ± 0.6
1	128.8 ± 6.1
5	96.0 ± 1.9
10	89.3 ± 1.4

Note. 3T3-L1 cultures were treated with 1, 5, or 10 μM $HgCl_2$ throughout differentiation. On day 7, 3T3-L1 adipocytes were fixed, stained with Nile Red, and analyzed by flow cytometry to determine the mean fluorescence of Nile Red in $HgCl_2$-treated and untreated adipocytes. Data are presented as the mean ± standard error from the mean with significant differences represented by different superscripts (ANOVA, $p < 0.05$).

differentiation (Ntambi and Young-Cheul, 2000). $HgCl_2$ dose-dependently decreased expression of PPARγ up to 70 and 95% in 3T3-L1 and 10T1/2 cells, respectively (Fig. 3). GLUT 4 is not detected in 3T3-L1 or 10T1/2 fibroblasts, however, expression increases in the maturation phase of adipogenesis, making it useful as a marker of late differentiation (Resh, 1982). We hypothesized that the reduced number of phenotypic adipocytes would correlate with lower expression of GLUT 4. Treatment with 10 μM $HgCl_2$ inhibited the expression of GLUT 4 in 10T1/2 cells; however, total GLUT 4 expression in 3T3-L1 cells did not change with $HgCl_2$ treatment (Fig. 4). These data show that $HgCl_2$ inhibits expression of proteins critical for both the commitment and maturation of these cells to adipocytes, but that models can differ in their response to $HgCl_2$.

$HgCl_2$ Affects the Phosphorylation of Kinases Associated with Adipocyte Differentiation and Metabolism

The hormonal stimulus used to differentiate these two mouse embryo fibroblast cell lines elicits a cascade of cell signaling events involved in regulating the process. The potential for $HgCl_2$ exposure to modify several important signaling proteins, including ERK1/2 and JNK, was determined for both cell lines. To avoid activation of signaling proteins by the addition of fresh serum to the culture, a modified differentiation protocol was used in which the hormones were added directly to the media present in the culture. As expected based on previous reports (Prusty *et al*., 2002), insulin and the differentiation cocktail caused an increase in ERK phosphorylation in both cell lines (Fig. 5). $HgCl_2$ treatment had no significant effect on the amount of ERK phosphorylation in either the 10T1/2 or 3T3-L1 cell line at 10 min (Fig. 5). In 10T1/2 cells, phosphorylated JNK was detected at 10 min and 1 h in cells treated with insulin or IDM/BRL, in the presence and absence of $HgCl_2$, suggesting that $HgCl_2$ has no effect on JNK at these early time points. However, $HgCl_2$ does have an effect at later time points. At 6 h, JNK phosphorylation was only detected in 10T1/2 cells that were treated with $HgCl_2$ (alone or with hormones). In contrast, phosphorylated JNK was not detected in 3T3-L1 cells until 6 h in cells treated with insulin alone and insulin with $HgCl_2$.

Effect of $HgCl_2$ on Insulin-Stimulated Glucose Transport

We next hypothesized that insulin-stimulated glucose transport would be indicative of the changes in GLUT 4 expression reported above (Fig. 4). Thus, insulin-stimulated glucose transport would decrease in 10T1/2 cells treated with $HgCl_2$ and remain unchanged in 3T3-L1 cells that maintain levels of GLUT 4 expression. Insulin-mediated glucose uptake is a characteristic of adipocytes that is acquired during differentiation with the concomitant increase in expression of insulin-responsive transporter GLUT 4 (Resh, 1982). The effect of $HgCl_2$ on insulin-mediated uptake was measured in the 10T1/2 and 3T3-L1 adipocytes after differentiation in the presence and absence of $HgCl_2$ (Fig. 6). Basal glucose uptake increased dose-dependently in $HgCl_2$-treated 3T3-L1 adipocytes. In addition to the change in basal glucose uptake with $HgCl_2$, insulin-mediated glucose uptake decreased in cells treated with $HgCl_2$ during differentiation in a dose-dependent manner (Fig. 6). For example, insulin stimulated glucose uptake 3-fold in untreated 3T3-L1 adipocytes but only 1.3-fold in cells treated with 5 μM $HgCl_2$ during differentiation. In contrast, differentiated 10T1/2 cells were poorly insulin responsive (independent of treatments), although they did demonstrate an $HgCl_2$-induced increase in basal glucose uptake like 3T3-L1 adipocytes. $HgCl_2$ did not appear to have an effect on insulin-mediated glucose transport in 10T1/2 adipocytes; however, their poor insulin response may have precluded observing such an effect.

DISCUSSION

Adipogenesis is an intricate, well-controlled process that has been studied extensively *in vitro* and *in vivo*. However, microarray analysis reveals distinct transcriptional profiles of adipogenesis *in vivo* and *in vitro* (Soukas *et al*., 2001). Differences in gene expression *in vivo* and *in vitro* emphasize the importance of studying multiple *in vitro* model systems, each of which may shed light on important aspects of *in vivo* differentiation. Therefore, we examined two cell models to address the hypothesis that $HgCl_2$ inhibits adipogenesis.

$HgCl_2$ dose-dependently inhibits adipogenesis in both 3T3-L1 and C3H10T1/2 cells (Fig. 1). The mechanism through which $HgCl_2$ inhibits adipocyte differentiation has yet to be defined; however, we present evidence that the disruption of transcription factor expression and insulin-signaling pathways may be involved. There are two phases of differentiation: commitment and maturation. Disruption of differentiation can occur during one or both of these phases. For example, previous studies showed that retinoic acid and TCDD decrease adipogenesis when present during the commitment phase but not when present during the maturation phase (Phillips *et al*.,

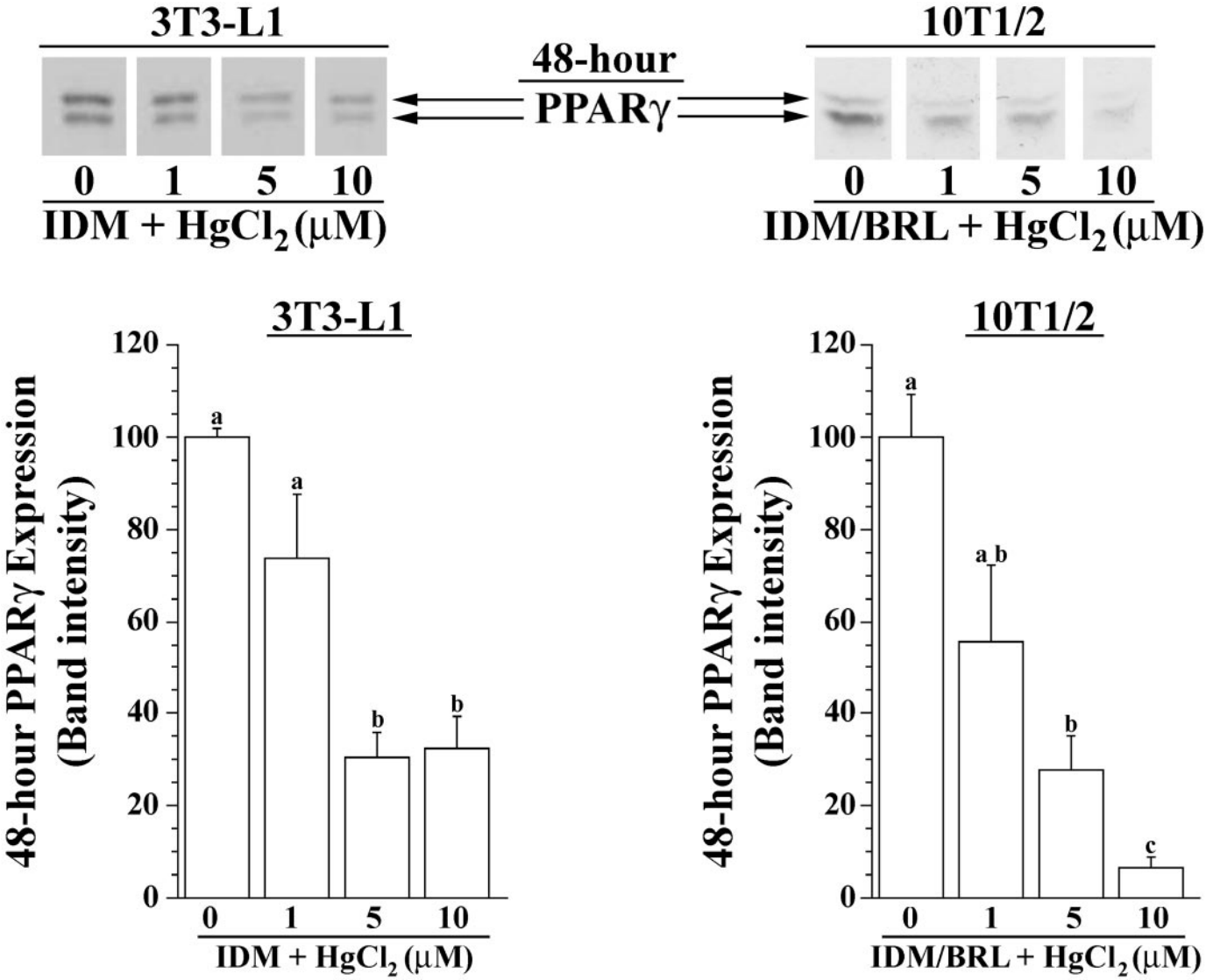

FIG. 3. The effect of $HgCl_2$ on PPARγ expression in 3T3-L1 and 10T1/2 cells as shown by representative experiments where IDM or IDM/BRL was added to confluent 3T3-L1 or 10T1/2 cells, respectively. $HgCl_2$ was added concurrently at 1, 5, and 10 μM and cell lysates were collected 48 h after treatment. Next, 80 μg of total cell lysate protein was separated by SDS-PAGE and analyzed by immunoblotting with a monoclonal antibody for PPARγ. Western blots from one representative experiment are shown from a set of triplicate independent cultures. PPARγ expression levels were quantitated by image analysis. Results are normalized to IDM or IDM/BRL-stimulated levels (set to 100) and reported below blots. Data are presented as the mean $\pm$ SE of the mean. Columns with different letters (abc) are significantly different from one another (ANOVA, $p < 0.05$).

1995; Xue *et al*., 1996). Similarly we have demonstrated that while the timing of $HgCl_2$ exposure has different effects on adipocyte differentiation in the two cell lines (e.g., $HgCl_2$ is more effective during the commitment phase in 10T1/2), $HgCl_2$ inhibited adipogenesis when present in one or both phases of differentiation. Our data indicate that, while $HgCl_2$ treatment inhibits adipogenesis in both cell lines, different mechanisms are at work in the different cell lines and may explain differences of other end points between the two cell lines (e.g., GLUT 4 expression and insulin-mediated glucose transport).

Previous studies have shown that the inhibition of PPARγ expression inhibits differentiation (Gurnell *et al*., 2000). Figure 3 shows that, at 48 h (peak PPARγ expression), $HgCl_2$ dose-dependently reduced PPARγ expression in both 3T3-L1 and 10T1/2 cells. However, decreased expression of PPARγ during the commitment phase alone does not appear to be responsible for the actions of $HgCl_2$ because the addition of $HgCl_2$ after 48 h (after commitment phase) still reduced differentiation of both cell types.

Insulin is the only component of the differentiation cocktail that is present throughout adipocyte commitment and maturation. Since $HgCl_2$ inhibited adipocyte differentiation when added during either phase of differentiation, the interactions

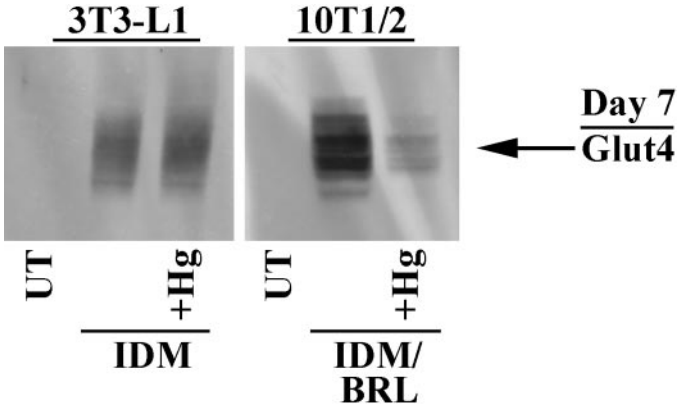

FIG. 4. The effect of $HgCl_2$ on GLUT 4 expression as shown by representative experiments where 3T3-L1 and 10T1/2 cells were differentiated in the presence and absence of 10 μM $HgCl_2$. On day 7, cell lysates were collected as described in Materials and Methods. Then, 80 μg of total cell lysate was analyzed by immunoblotting with a polyclonal antibody that specifically recognizes GLUT 4.

with insulin responses were closely examined. Insulin activates kinases important for adipocyte differentiation and function including extracellular receptor kinase (ERK), which is phosphorylated in response to insulin and activated by metals such as zinc (Tang and Shay, 2000), vanadate, and arsenic (Wu *et al*., 1999). The action of $HgCl_2$ on the ERK phosphorylation is not well documented. Figure 5 shows that ERK phosphorylation is associated with the initiation of differentiation in both cell lines. $HgCl_2$, however, had no effect on ERK phosphorylation, suggesting that ERK is not a target of $HgCl_2$ in the inhibition of adipogenesis. While there is some controversy as to whether ERK activity is required for adipocyte differentiation (De Mora *et al*., 1997; Qiu *et al*., 2001), ERK activity is required for the environmental contaminant TCDD to inhibit adipocyte differentiation (Hanlon *et al*., 2003).

SAPK family member c-Jun N-terminal kinase (JNK) regulates adipocyte differentiation and function of mature adipocytes (Camp *et al*., 1999). Although it is not directly activated by insulin, it can contribute to the downregulation of the insulin signal by serine phosphorylation of insulin receptor substrate 1 (IRS-1; Aguirre *et al*., 2000). Serine phosphorylation of IRS-1 results in decreased phosphorylation of IRS-1 downstream targets, which has been linked to insulin resistance (Zick, 2001). In addition to JNK action on insulin-signaling pathways, active JNK also phosphorylates PPARγ, thereby inhibiting its transcriptional activity (Camp *et al*., 1999). Reduced activity would lead to decreased adipocyte differentiation and, while we observed a decrease in PPARγ expression, reduced activity may also contribute to the $HgCl_2$-mediated inhibition of differentiation. $HgCl_2$ treatment has been shown to stimulate JNK activity in other cell systems including rabbit renal cortical slices (Turney *et al*., 1999) and LLC-PK cells (Matsuoka *et al*., 2000), although the physiological consequences of JNK phosphorylation in these cells were not examined. We report here that $HgCl_2$ treatment had no effect on JNK phosphorylation in 3T3-L1 cells. However, in 10T1/2 cells, $HgCl_2$ exposure led to a prolonged phosphorylation of JNK, which occurred independently of the presence of any hormones. If this prolonged JNK phosphorylation leads to serine phosphorylation of IRS-1 and subsequent inactivation, insulin signaling would be disrupted. Since insulin signaling is required for both the commitment to and maturation of adipocytes, downregulation of insulin signaling via JNK activation is a possible mechanism through which $HgCl_2$ inhibits adipogenesis.

In addition to the molecular data showing $HgCl_2$ disrupts signaling pathways used by insulin, we present physiological data that shows there is a decrease in insulin-mediated glucose transport in cells differentiated in the presence of $HgCl_2$. Figure 6 shows that 3T3-L1 cells treated with $HgCl_2$ during differentiation reduced insulin-mediated glucose transport dose-dependently. This may be due to fewer adipocytes, reduced expression of the insulin-responsive glucose transporter, disruption of normal insulin-signaling pathways, or some combination of these events. The reduction in adipocyte number was about 50% for 3T3-L1 cells treated with 5 μM $HgCl_2$ (Fig. 1A). $HgCl_2$ treatment decreased insulin-mediated glucose uptake 2.8-fold (700 to 250 pmole/well for control and 5 μM

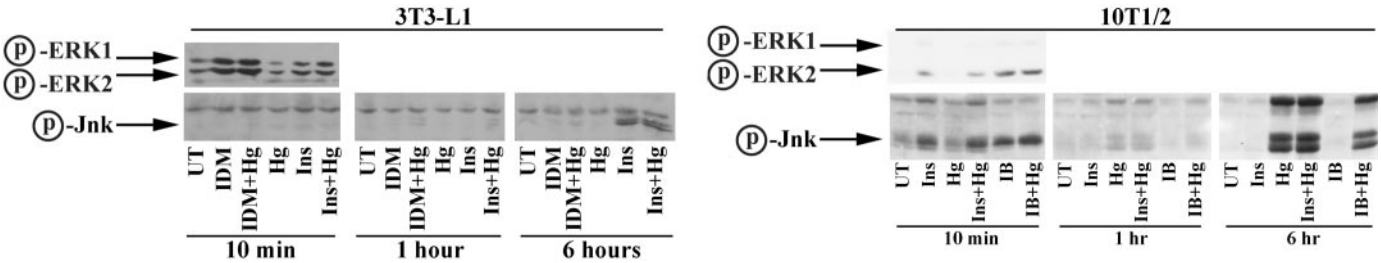

FIG. 5. The effect of $HgCl_2$ on JNK and ERK phosphorylation is shown. When 3T3-L1 and 10T1/2 cells reached confluence, they were induced to differentiate with IDM or IDM/BRL, respectively, as described in Materials and Methods. Next, 10 μM $HgCl_2$ was added concurrently with IDM or IDM/BRL; 10 min, 1 h, and 6 h after treatment, cells were harvested as described in Materials and Methods. Then, 80 μg of total cell lysate was analyzed by immunoblotting with polyclonal antibodies that specifically recognize the phosphorylated forms of JNK and ERK. UT, untreated; IDM or IB, normal differentiation cocktail; Ins, insulin.

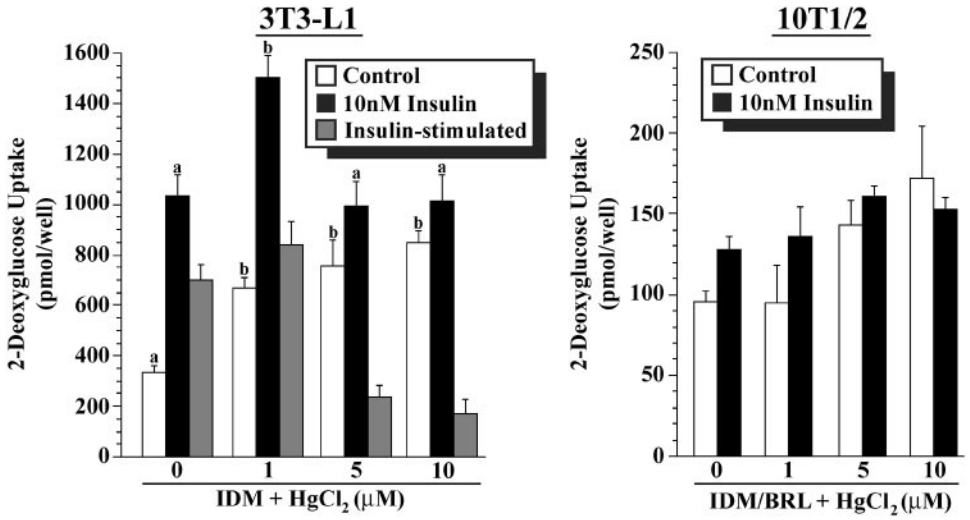

FIG. 6. The effect of $HgCl_2$ on basal and insulin-mediated uptake of ^{3}H-deoxyglucose in 3T3-L1 and 10T1/2 cells is shown. Cells were incubated with the indicated concentrations of $HgCl_2$ during differentiation (days 0–7 and 0–2 for 3T3-L1 and 10T1/2 cells, respectively). Following differentiation, cells were serum starved for 2 h and the uptake of 50 μM ^{3}H-2-deoxyglucose was measured in the presence and absence of an insulin stimulus (10 nM). Cells were washed twice with KRPH buffer and incubated in KRPH for 1 h. Deoxyglucose uptake was measured during the last 10 min of KRPH incubation. Data are presented as the mean value of four replicate wells with variability shown as standard error from the mean. Columns with different letters (abc) within a treatment are significantly different from one another (ANOVA, $p < 0.05$). Insulin-stimulated deoxyglucose uptake was calculated by subtracting deoxyglucose uptake in treated and untreated cells from their respective insulin-treated counterpart.

$HgCl_2$ respectively), suggesting adipocyte number alone would not account for the reduced insulin responsiveness. Although GLUT 4 expression decreased in $HgCl_2$-treated 10T1/2 cells, no difference was observed in 3T3-L1 cells; yet, $HgCl_2$-treated 3T3-L1 adipocytes exhibited insulin resistance. Insulin resistance, characterized as a decreased response of insulin-sensitive tissues to the hormonal stimulus, is a metabolic condition contributing to Type 2 diabetes. Insulin resistance can be induced by numerous factors including elevated levels of TNF-α and free fatty acids (Zick, 2001). Ryden and coworkers (2002) showed that, in the adipocyte, TNF-α induces insulin resistance, in part, through the activation of the MAPK pathway including rapid phosphorylation of JNK, suggesting that exposure to chemicals that induce phosphorylation of JNK may contribute to the onset of insulin resistance.

Insulin resistance is a condition that contributes to the onset of noninsulin-dependent diabetes mellitus (NIDDM or Type II diabetes; Zimmet *et al*., 2001). Many conditions have been shown to induce insulin resistance in *in vitro* cell culture models including oxidative stress (Rudich *et al*., 1997) and exposure to TNF-α (Engelman *et al*., 2000). Additionally, exposure to two environmental toxins, arsenic and TCDD, has been linked to an increased incidence of insulin resistance in epidemiological studies (Lai *et al*., 1994; Longnecker and Michalek, 2000). TCDD and arsenic have also been shown to inhibit adipogenesis in cell culture models (Hanlon *et al*., 2003; Trouba *et al*., 2000). The data presented in this report demonstrate that $HgCl_2$ inhibits adipogenesis in two models of adipocyte differentiation, raising the question of whether exposure to $HgCl_2$ contributes to the onset of insulin resistance. Epidemiological studies of people living in methyl mercury–(MeHg-) contaminated areas indicate no correlation of exposure to MeHg and the onset of diabetes (Futatasuka *et al*., 1996, 2000). However, comparisons between the action of MeHg and $HgCl_2$, forms of mercury with different chemical characteristics and metabolic actions, on glucose homeostasis and adipogenesis have not been examined. Previous research has demonstrated that the effects of MeHg and $HgCl_2$ differ in neuronal cell differentiation (Parran *et al*., 2001) and in calcium regulation in T lymphocytes (Tan *et al*., 1993). Further comparisons among different forms of mercury are necessary to determine their potential contribution to pathologies associated with glucose homeostasis.

Mercury exposure does not appear to be a contributing factor in the less common form of diabetes, insulin-dependent diabetes mellitus (IDDM). Exposure to $HgCl_2$ was shown to have no effect on the incidence of IDDM in diabetes-prone rats (Kosuda *et al*., 1997). However, exposure to $HgCl_2$ delays the onset of IDDM in a nonobese diabetic mouse model of diabetes as measured by glucosuria (Brenden *et al*., 2001). Thus, there are recognized effects of $HgCl_2$ on systems contributing to diabetes, although effects on the most prevalent from, NIDDM, remain unclear. $HgCl_2$ is a prevalent environmental toxicant that has been recognized to have serious impacts on human health (U.S. EPA, 1997); however, little research has been done on the effects of $HgCl_2$ on adipocyte function. This study provides evidence that environmental levels of $HgCl_2$ may be a contributing factor to the onset of insulin resistance and, potentially, Type II diabetes mellitus.

ACKNOWLEDGMENTS

This study was supported by grant R825218 from the U.S. EPA (D. M. B.), NIH grant RO1 DK55302 (C. R. Jefcoate), and by grant number T32 ES07015 from the National Institute of Environmental Health Sciences (NIEHS), NIH. Its contents are solely the responsibility of the authors and do not necessarily represent the official views of the NIEHS/NIH.

REFERENCES

Aguirre, V., Uchida, T., Yenush, L., Davis, R., and White, M. F. (2000). The c-Jun NH_2-terminal kinase promotes insulin resistance during association with insulin receptor substrate-1 and phosphorylation of Ser^{307}. *J. Biol. Chem.* **275,** 9047–9054.

Alexander, D. L., Ganem, L. G., Fernandez-Salguero, P., Gonzalez, F., and Jefcoate, C. R. (1998). Aryl-hydrocarbon receptor is an inhibitory regulator of lipid synthesis and of commitment to adipogenesis. *J. Cell Sci.* **111,** 3311–3322.

Barnes, D. M., Sykes, D. B., and Miller, D. S. (1999). Multiple effects of mercuric chloride on hexose transport in Xenopus oocytes. *Biochim. Biophys. Acta.* **1419,** 289–298.

Brenden, N., Rabbani, H., and Abedi-Valugerdi, M. (2001). Analysis of mercury-induced immune activation in nonobese diabetic (NOD) mice. *Clin. Exp. Immunol*. **125,** 202–210.

Camp, H. S., Tafuri, S. R., and Leff, T. (1999). c-Jun N-terminal kinase phosphorylates PPARγ1 and negatively regulates its transcriptional activity. *Endocrinology* **140,** 392–397.

De Mora, J. F., Porras, A., Ahn, N., and Santos, E. (1997). Mitogen-activated protein kinase activation is not necessary for, but antagonizes, 3T3–L1 adipocytic differentiation. *Mol. Cell. Biol.* **17,** 6068–6075.

Dubyak, G. R., and Kleinzeller, A. (1980). The insulin-mimetic effects of vanadate in isolated rat adipocytes. Dissociation from effects of vanadate as a (Na+-K+)ATPase inhibitor. *J. Biol. Chem*. **255,** 5306–5312.

Engelman, J. A., Berg, A. H., Lewis, R. Y., Lisanti, M. P., and Scherer, P. E. (2000). Tumor necrosis factor alpha–mediated insulin resistance, but not dedifferentiation, is abrogated by MEK1/2 inhibitors in 3T3–L1 adipocytes. *Mol. Endocrinol.* **14,** 1557–1569.

Ezaki, O. (1989). IIb group metal ions (Zn^{2+}, Cd^{2+}, Hg^{2+}) stimulate glucose transport activity by post-insulin receptor kinase mechanism in rat adipocytes. *J. Biol. Chem.* **264,** 16118–16122.

Frost, S. C., and Lane, M. D. (1985). Evidence for the involvement of vicinal sulfhydryl groups in insulin-activated hexose transport by 3T3–L1 adipocytes. *J. Biol. Chem.* **260**(5), 2646–2652.

Futatsuka, M., Kitano, T., Shono, M., Fukuda, Y., Ushijima, K., Inaoka, T., Nagano, M., Wakamiya, J., and Miyamoto, K. (2000). Health surveillance in the population living in a methyl mercury–polluted area over a long period. *Environ. Res.* **83,** 83–92.

Futatsuka, M., Kitano, T., and Wakamiya, J. (1996). An epidemiological study on diabetes mellitus in the population living in a methyl mercury polluted area. *J. Epidemiol*. **6,** 204–208.

Gurnell, M., Wentworth, J. M., Agostini, M., Adams, M., Collingwood, T. N., Provenzano, C., Browne, P. O., Rajanayagam O., Burris, T. P., Schwabe, J. W., *et al.* (2000). A dominant-negative peroxisome proliferator-activated receptor (PPAR) mutant is a constitutive repressor and inhibits PPAR-mediated adipogenesis. *J. Biol. Chem.* **275,** 5754–5759.

Hanlon, P. R., Ganem, L. G., Cho, Y. C., Yamamoto, M., and Jefcoate, C. R. (2003). AhR- and ERK-dependent pathways function synergistically to mediate 2,3,7,8-tetrachlorodibenzo-p-dioxin suppression of peroxisome proliferator-activated receptor-gamma1 expression and subsequent adipocyte differentiation. *Toxicol. Appl. Pharmacol*. **189,** 11–27.

Harrison, S. A., Buxton, J. M., Clancy, B. M., and Czech, M. P. (1991). Evidence that erythroid-type glucose transporter intrinsic activity is modulated by cadmium treatment of mouse 3T3–L1 cells. *J. Biol. Chem.* **266,** 19438–19449.

Jin, S., Zhai, B., Qiu, Z., Wu, J., Lane, M. D., and Liao, K. (2000). c-Crk, a substrate of the insulin-like growth factor-1 receptor tyrosine kinase, functions as an early signal mediator in the adipocyte differentiation process. *J. Biol. Chem.* **275,** 34344–34352.

Kosuda, L. L., Greiner, D. L., and Bigazzi, P. E. (1997). Effects of $HgCl_2$ on the expression of autoimmune responses and disease in diabetes-prone (DP) BB rats. *Autoimmunity* **26,** 173–187.

Lai, M. S., Hsueh, Y. M., Chen, C. J., Shyu, M. P., Chen, S. Y., Kuo, T. L., Wu, M. M., and Tai, T. Y. (1994). Ingested inorganic arsenic and prevalence of diabetes mellitus. *Am. J. Epidemiol.* **139,** 484–492.

Liao, K., and Lane, M. D. (1995). The blockade of preadipocyte differentiation by protein-tyrosine phosphatase HA2 is reversed by vanadate. *J. Biol. Chem.* **270,** 12123–12132.

Longnecker, M. P., and Michalek, J. E. (2000). Serum dioxin level in relation to diabetes mellitus among Air Force veterans with background levels of exposure. *Epidemiology* **11**(1), 44–48.

Matsuoka, M., Wispriyono, B., Iryo, Y., and Igisu, H. (2000). Mercury chloride activates c-Jun N-terminal kinase and induces *c-jun* expression in LLC-PK cells. *Toxicol. Sci.* **53,** 361–368.

May, J. M., and Contoreggi, C. S. (1982). The mechanism of the insulin-like effects of ionic zinc. *J. Biol. Chem.* **257,** 4362–4368.

Moreno-Aliaga, M. J., and Matsumura, F. (1999). Endrin inhibits adipocyte differentiation by selectively altering expression pattern of CCAAT/enhancer binding protein-alpha in 3T3–L1 cells. *Mol. Pharmacol.* **56,** 91–101.

Ntambi, J. M., and Young-Cheul, K. (2000). Adipocyte differentiation and gene expression. *J. Nutr.* **130,** 3122S–3126S.

Parran, D. K., Mundy, W. R., and Barone, S. (2001). Effects of methylmercury and mercuric chloride on differentiation and cell viability in PC12 cells. *Toxicol. Sci.* **59,** 278–290.

Phillips, M., Enan, E., Phillip, C., Liu, C., and Matsumura, F. (1995). Inhibition of 3T3–L1 adipose differentiation by 2,3,7,8-tetrachlorodibenzo-p-dioxin. *J. Cell Sci.* **108,** 395–402.

Prusty, D., Park, B. H., Davis, K. E., and Farmer, S. R. (2002). Activation of MEK/ERK signaling promotes adipogenesis by enhancing peroxisome proliferator-activated receptor gamma (PPARγ) and C/EBPalpha gene expression during the differentiation of 3T3–L1 preadipocytes. *J. Biol. Chem.* **277**(48), 46226–46232.

Qiu, Z., Wei, Y., Chen, N., Jiang, M., Wu, J., and Liao, K. (2001). DNA synthesis and mitotic clonal expansion is not a required step for 3T3–L1 preadipocyte differentiation into adipocytes *J. Biol. Chem.* **276,** 11988–11995.

Resh, M. D. (1982). Development of insulin responsiveness of the glucose transporter and the (Na^+, K^+)-adenosine triphosphatase during *in vitro* adipocyte differentiation. *J. Biol. Chem.* **257,** 6978–6986.

Rudich, A., Kozlovsky, N., Potashnik, R., and Bashan, N. (1997). Oxidant stress reduces insulin responsiveness in 3T3–L1 adipocytes. *Am. J. Physiol.* **272**(5 Pt 1), E935–E940.

Ryden, M., Dicker, A., van Harmelen, V., Hauner, H., Brunnberg, M., Perbeck, L., Lonnqvist, F., and Arner, P. (2002). Mapping of early signaling events in tumor necrosis factor-alpha–mediated lipolysis in human fat cells. *J. Biol. Chem.* **277**(2), 1085–1091.

Shao, D., and Lazar, M. A. (1997). Peroxisome proliferator activated receptor γ, CCAAT/enhancer-binding protein α, and cell cycle status regulate the commitment to adipocyte differentiation. *J. Biol. Chem.* **272,** 21473–21478.

Shechter, Y., and Ron, A. (1986). Effect of depletion of phosphate and bicarbonate ions on insulin action in rat adipocytes. *J. Biol. Chem.* **261,** 14945–14950.

Soukas, A., Socci, N. D., Saatkamp, B. D., Novelli, S., and Friedman, J. M. (2001). Distinct transcriptional profiles of adipogenesis *in vivo* and *in vitro*. *J. Biol. Chem.* **276**(36), 34167–34174.

Tan, X. X., Tang, C., Castoldi, A. F., Manzo, L., and Costa, L. G. (1993). Effects of inorganic and organic mercury on intracellular calcium levels in rat T lymphocytes. *J. Toxicol. Environ. Health* **38,** 159–170.

Tang, X., and Shay, N. F. (2001). Zinc has an insulin-like effect on glucose transport mediated by phosphoinositol-3-kinase and Akt in 3T3–L1 fibroblasts and adipocytes. *J. Nutr.* **131,** 1414–1420.

Trouba, K. J., Wauson, E. M., and Vorce, R. L. (2000). Sodium arsenite inhibits terminal differentiation of murine C3H 10T1/2 preadipocytes. *Toxicol. Appl. Pharmacol.* **168**(1), 25–35.

Turney, K. D., Parrish, A. R., Orozco, J., and Gandolfi, A. J. (1999). Selective activation in the MAPK pathway by Hg(II) in precision-cut rabbit renal cortical slices. *Toxicol. Appl. Pharmacol.* **160,** 262–270.

U.S. Environmental Protection Agency (U.S. EPA) (1997). Executive summary, vol. 1. In *Environmental Protection Agency (U.S.). Mercury Study Report to Congress*, Pub. No.: EPA-425/R, pp. 97–103. EPA, Washington, DC.

Wauson, E. M., Langan, A. S., and Vorce, R. L. (2002). Sodium arsenite inhibits and reverses expression of adipogenic and fat cell-specific genes during *in vitro* adipogenesis. *Toxicol. Sci.* **65,** 211–219.

Wu, W., Graves, L. M., Jaspers, I., Devlin, R. B., Reed, W., and Samet, J. M. (1999). Activation of the EGF receptor signaling pathway in human airway epithelial cells exposed to metals. *Am. J. Physiol.* **277**(5 Pt 1), L924–L931.

Xue, J. C., Schwarz, E. J., Chawla, A., and Lazar, M. A. (1996). Distinct stages in adipogenesis revealed by retinoid inhibition of differentiation after induction of PPARγ. *Mol. Cell. Biol.* **16,** 1567–1575.

Zick, Y. (2001). Insulin resistance: A phosphorylation-based uncoupling of insulin signaling. *Trends Cell Biol.* **11,** 437–441.

Zimmet, P., Alberti, K. G. M. M., and Shaw, J. (2001). Global and societal implications of the diabetes epidemic. *Nature* **414,** 782–787.